Kinetics and Catalysis, Vol. 44, No. 4, 2003, pp. 555–561. Translated from Kinetika i Kataliz, Vol. 44, No. 4, 2003, pp. 607–613.
Original Russian Text Copyright © 2003 by Rostovshchikova, Smirnov, Kozhevin, Yavsin, Gurevich.

HIGHLY ORGANIZED CATALYTIC SYSTEMS

Structurally Organized Nanocomposites in the Catalysis of Chlorohydrocarbon Reactions

T. N. Rostovshchikova*, V. V. Smirnov*, V. M. Kozhevin, D. A. Yavsin**, and S. A. Gurevich****

** Department of Chemistry, Moscow State University, Moscow, 119992 Russia*

*** Ioffe Physicotechnical Institute, Russian Academy of Sciences, St. Petersburg, 194021 Russia*

Received September 3, 2002

Abstract—Catalysis by closely packed metal films containing monodispersed nanocluster ensembles was considered using the reactions of chlorinated hydrocarbons as an example; these reactions include a step of electron transfer from a catalyst to a reactant. A new laser electrodispersion technique was used for preparing films that consisted of spherical copper grains 5 nm in size coated with thin (0.7 nm) layers of copper(I) oxide with different particle packing densities on the surface of thermally oxidized silicon. A comparison of the catalytic activity of films with varied packing density in media with different permittivities allowed us to assume that the observed maximum activity of closely packed films was associated with the appearance of charged grains in the ensembles of interacting nanoparticles due to the thermal fluctuations of electrons between closely spaced grains.

INTRODUCTION

The development of new procedures for the synthesis of stable nanoparticles with a specified size provides an opportunity to understand the reasons for the dramatic difference between the physical, electronic, and catalytic properties of giant clusters (from 2–3 nm to several tens of nanometers) and, on the one hand, bulk metals or, on the other hand, isolated atoms and small clusters. Size effects in catalysis by nanoparticles are associated with a number of factors. The most important of these factors consists in changes in the energy of electronic levels, particle morphology (in particular, the contribution of elements of various crystallographic planes), specific surface area, and the number and character of defects [1–3]. The frequently considered hypothesis that an increase in the surface of metal upon dispersion plays a predominant role in increasing catalytic ability cannot explain the anomalously high catalytic activity of nanosystems, which manifests itself at a precisely specified composition. Thus, in the catalysis of chlorohydrocarbon reactions by Pd [4], Cu [5, 6], and Fe [7] nanoparticles stabilized in polymer matrices, an extremal change in the catalytic properties of nanocomposites (activity or selectivity) with metal content was found; this primarily resulted in a decrease in distances between particles. It is likely that special properties of the nanocluster–support or matrix systems significantly depend on the organization of nanoparticles on the surface or in the matrix, which is responsible for the interaction of particles with each other and for the appearance of new physicochemical properties in the ensembles of interacting clusters. Hence, it follows that the average distances *L* between nanoclusters can play an important role in the formation of special properties of nanoparticle systems. From threshold values of *L*, electron transfer between closely spaced metal particles takes place in polymer matrices to result in the mutual charging [8, 9]. Many catalytic reactions of halogenated hydrocarbons include a step of electron transfer from the catalyst to the substrate [10, 11]; therefore, the appearance of negatively charged particles will strongly affect the catalytic properties of the system. The hypothesis that charge transfer between interacting nanoclusters in catalysis plays an important role was supported by the fact that the maximum of catalytic activity coincided with a conductivity jump in metal–polymer composites [8, 9].

Summarizing the results of studies on metal–polymer nanocomposites, we can formulate the conclusions given below. In our opinion, they are required in order to adequately describe catalysis by the systems of interacting nanoparticles.

(1) Along with the well-known size effect, the dependence of catalytic activity on the intrinsic size of nanoparticles (we designate it as the size effect of the first kind), there is another type of size effect (we designate it as the size effect of the second kind) due to the dependence of catalytic properties on the distance *L* between nanoparticles.

(2) The size effect of the second kind manifests itself on attaining a minimally required threshold value of *L*, when electron redistribution between closely spaced particles becomes possible. We designate nanocluster groups in which this distribution takes place as nanocluster ensembles.

(3) If considerable electron-density redistribution between the catalyst and reaction substrates occurs in the transition sate of a rate-limiting step of the reaction (i.e., if the reaction is sensitive to the charge on the cat-

alyst), the appearance of ensembles will result in a dramatic increase in the catalytic activity. As the metal content is increased beyond the optimum value, the enlargement of clusters and the formation of extended conducting metal aggregates decrease the charge density on the surface of nanoparticles and, correspondingly, the catalytic activity.

However, the metal particle size and shape distributions in metal–polymer composites and the necessity of taking into account the chemical interaction of the metal with the polymer (for example, see [7]) make the results difficult to interpret. To distinguish between size effects of different origins, data on stable monodispersed systems are required, which provide an opportunity to ignore both the effects of metal particle size and shape and the metal–polymer chemical interaction. The relationship between the catalytic properties and the distance L between nanoparticles can be revealed only under the above conditions. Thus, the aim of this work was to detect a size effect of the second kind, that is, to determine the effect of distance between nanoparticles on the catalytic properties of immobilized nanoclusters.

Based on the above concepts, the reaction rate would be expected to be an extremal function of L even in the case of particles with the same sizes and shapes. Factors that facilitate the formation of charged particles, for example, an increase in the permittivity of the medium or in the temperature, should enhance the catalytic properties of nanoparticle ensembles.

The use of laser electrodispersion, which is a recently developed new technique for the production of monodispersed metal nanoparticle systems, made it possible to compare the catalytic properties of isolated nanoparticles and nanoparticle ensembles under conditions when particle size and shape remained unchanged and the particles did not interact with the matrix. Laser electrodispersion was described in detail elsewhere [12]. A fundamental characteristic of this technique is that metal droplets with a specified size preformed in a laser plasma torch are deposited onto a support to produce spherical nanoparticles immobilized on the surface of the support with a narrow size distribution (the deviation was within ±20%). The particle size depends only on the nature of the metal. It is 5 nm for copper. At the stage of condensation, metal nanodroplets bear a negative charge, which was acquired in the laser plasma torch. Because of this, the coagulation of aggregates on the surface of the support does not occur until almost complete surface coverage and the onset of growth of the second layer of nanoclusters. The micrograph (Fig. 1) demonstrates a typical example of closely packed copper nanoclusters on the surface of oxidized silicon. At the surface density of particles $n = 4 \times 10^{12}$ cm^{-2}, the majority of spherical grains formed islands of closely contacting particles. The distance between the metal nuclei of nanoclusters was 1.5 nm, which is approximately equal to the doubled thickness of an oxide layer. At lower surface coverages, the variation of the amount of the metal resulted in a change in L at constant particle size and shape; this makes it possible to detect the size effect of the second kind.

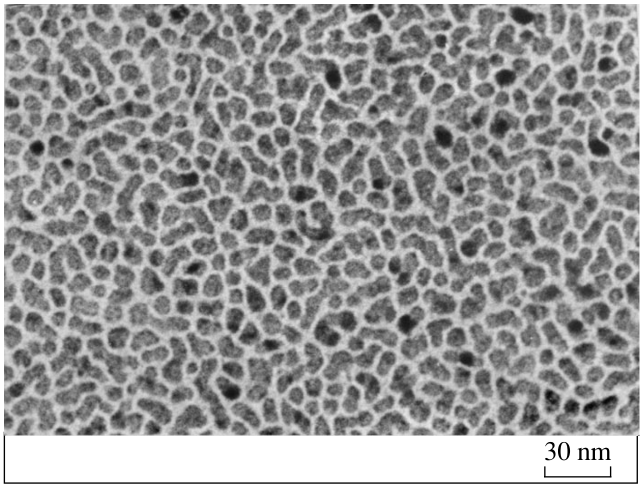

Fig. 1. Micrograph of a film with a deposition time of 5 min and the particle density $n = 4 \times 10^{12}$ particle/cm^2, which was obtained using a Philips EM420 transmission electron microscope.

To compare the catalytic properties of films with different surface concentrations of copper nanoparticles and, consequently, with different values of L, the following reactions were chosen as examples:

$$CH_2Cl{-}CHCl{-}CH{=}CH_2 \rightleftarrows CH_2ClCH{=}CHCH_2Cl \quad (I)$$

(the allyl isomerization of 3,4-dichloro-1-butene into *trans*-1,4-dichloro-2-butene);

$$CCl_4 + CH_3(CH_2)_5CH{=}CH_2 \longrightarrow CH_3(CH_2)_5CHCl{-}CH_2(CCl_3) \quad (II)$$

(the addition of carbon tetrachloride at the double bond);

$$RH + CCl_4 \longrightarrow RCl + CHCl_3, \quad (III)$$

where $R = C_{10}H_{21}$ (the combined metathesis of C–H and C–Cl bonds).

EXPERIMENTAL

Copper nanoparticles were prepared by laser electrodispersion [12]. Surface-oxidized silicon, which was prepared from silicon (100) single crystals by boiling in acetone and successively treating with hydrogen peroxide in acidic and alkaline media followed by washing and drying, was used as a support. The thickness of the oxide layer was 0.5 μm with a total support thickness of 300 μm. A copper target was irradiated using a YAG-Nd laser (λ = 1.06 μm) with a pulse duration of 30 ns and a pulse energy of 0.3 J. The resulting submicron liquid metal droplets were extracted from the target surface to the laser torch zone because of the development of the capillary instability of a molten layer under the action of a nonuniform electric field (1–3 kV). The cascade division of liquid droplets charged in a laser plasma torch resulted in the formation of spherical copper particles of size 5 nm and in the deposition of these particles onto the surface of the support. The amount of the deposited metal and, consequently, the particle density on the support were varied by changing the deposition time τ in the range from 0.2 to 15 min. Special calibration experiments were performed to demonstrate that the surface density of nanoparticles in this range was proportional to the duration of deposition. In this case, according to data obtained using transmission electron microscopy (TEM), the sample structure changed from a system of individual grains uniformly distributed over the surface ($\tau \le 1$ min) to islands consisting of several nanoclusters, which were isolated from each other, ($\tau \approx$ 5 min) and then to a uniform surface coverage with closely packed nanoparticles ($\tau \ge 5$ min). The distance between individual grain islands was no greater than 3 nm. The deposition time of 10–15 min corresponds to the onset of formation of the second metal layer on the surface of nanoparticles. An XPS study of the chemical composition of the particles demonstrated that, after contact with air, these were metal nuclei of size 3.5–4.0 nm coated with a thin cover (0.7 nm) of Cu_2O [12]. Correspondingly, the dielectric gap between the metal nuclei of closely packed nanograins was 1.5 nm. The long-term (2–3 months) keeping of films in air did not result in the deep oxidation of the metal. Films stored in an argon atmosphere were used in particular experiments.

The reaction mixtures containing 0.1–0.3 ml of a solution (1×10^{-4}–3×10^{-3} mol of a reactant) and 0.1–1.0 cm^2 of a crushed catalyst film ($3 \times 10^{-10} - 4 \times 10^{-9}$ mol Cu) were prepared by mixing the components in air or in a vacuum; reactions were performed in sealed glass ampules on heating with stirring. The amount of the catalyst for samples with copper contents lower than 4×10^{12} particle/cm^2 (deposition times shorter than 5 min) was increased to provide comparable metal contents in all the experiments. Decane, carbon tetrachloride, chloroform, or dichloroethane was used as a solvent; thus, the solvent permittivity ε was varied from 2 to 10. The volume ratio between the reactants and the solvent was 1 : 10 for isomerization (I), and the ratio between 1-octene, carbon tetrachloride, and the solvent was 1 : 5 : 5 for the reaction mixture of process (II). The composition of products was analyzed by chromatography on an LKhM-3700 chromatograph with a flame-ionization detector on an SE-30 column.

Oxidized silicon exhibited low catalytic activity in reactions (I)–(III). The yield of 1,4-dichloro-2-butene in isomerization (I) on silicon supports in the absence of the metal for 4 h was no higher than 2% at 110°C. At 130 and 150°C, the yields of 1,1,1,3-tetrachlorononane, the product of addition (II), were ~5 and 9%, respectively, whereas the yields of 2-chlorodecane, the product of metathesis (III), were 0.1 and 0.3%, respectively. In the subsequent calculations, the amount of products formed because of catalysis by the support was subtracted from the total experimental value.

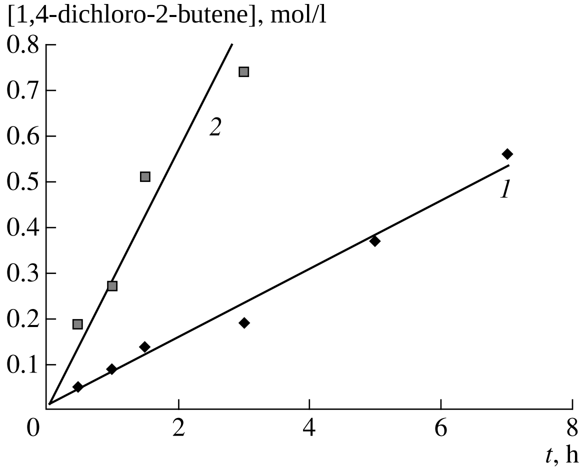

Fig. 2. Kinetic curves of 1,4-dichloro-2-butene buildup in the isomerization of 3,4-dichloro-1-butene (0.3 ml; 9.28 mol/l; 0.4 cm^2 of a catalyst film) at 100°C for films with a deposition time of 5 min and a particle density of 4×10^{12} particle/cm^2, which were stored (*1*) away from air or (*2*) in air.

RESULTS AND DISCUSSION

Dichlorobutene isomerization (I) occurred at 100–110°C; the rate of the reaction in the presence of copper nanoparticles supported on oxidized silicon was independent of the presence of oxygen in the reaction mixture. On the contrary, the conditions of film storage affected the rate of the reaction. This can be seen in Fig. 2, which demonstrates the kinetic curves of 1,4-dichloro-2-butene formation at 100°C for closely packed films (deposition time of 5 min; particle density of 4×10^{12} particle/cm^2), which were stored either away from air or in air. It follows from the above data that the initial rate of isomerization on copper nanoparticles that were kept away from air was lower than the rate in the presence of films stored in air by a factor of ~3. In the subsequent text, all data are given for films stored in air.

The reaction rate dramatically increased on changing from films with individual grains to closely packed films. Figure 3 demonstrates the kinetic curves of buildup of 1,4-dichloro-2-butene in isomerization (I) at 110°C for films with deposition times of 1, 2, and 5 min. The use of films with denser coverage as the deposition time was further increased did not result in an increase in the rate of isomerization. Another important characteristic of isomerization was an induction period, which disappeared in the reuse of the catalyst (Fig. 3, curve *4*).

The dilution of 3,4-dichloro-1-butene with nonpolar (carbon tetrachloride, ε = 2.24) and weakly polar sol-

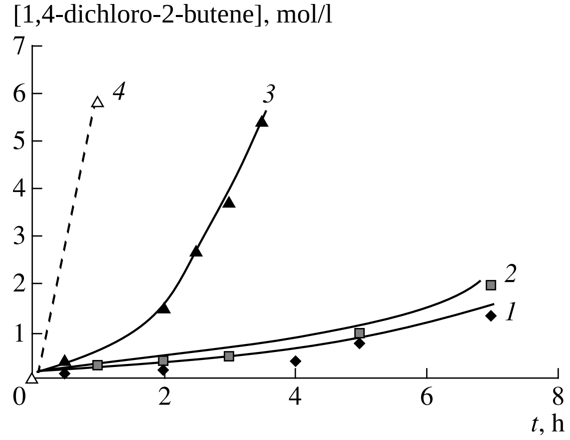

Fig. 3. Kinetic curves of 1,4-dichloro-2-butene buildup in the isomerization of 3,4-dichloro-1-butene (0.1 ml; 9.28 mol/l) at 110°C and different deposition times, copper particle densities on the support, and catalyst film sizes, respectively: (*1*) 1 min, 0.8×10^{12} particle/cm^2, and 1 cm^2; (*2*) 2 min, 1.6×10^{12} particle/cm^2, and 0.5 cm^2; (*3*) 5 min, 4.0×10^{12} particle/cm^2, and 0.2 cm^2; and (*4*) the reuse of sample *3*.

vents (chloroform, $\varepsilon = 5.05$) decreased the rate of isomerization, whereas the addition of the more polar solvent 1,2-dichloroethane ($\varepsilon = 10.03$) accelerated the process. Thus, the dilution of 3,4-dichloro-1-butene with dichloroethane in a ratio of 1 : 1 resulted in an increase in the yield of 1,4-dichloro-2-butene from 18 to 27% in 2 h at 110°C for a maximally active catalyst with $n = 4 \times 10^{12}$ particle/cm^2. Figure 4 demonstrates data on the specific activity of films in isomerization (I), which were calculated from reaction rates in various solvents (Table 1) as the amount of the product formed for an hour per the amount of copper. The dependence of the specific activity on the packing density of particles in dichloroethane, as well as in the case of pure 3,4-dichloro-1-butene ($\varepsilon \approx 8$–9), exhibited a pronounced maximum at $n = 4 \times 10^{12}$ particle/cm^2 for a closely packed film containing isolated grain aggregates (see Fig. 1). It can be seen that the accelerating effect of polarity was most pronounced at this packing density of nanoparticles on the support. The dependence of the rate of isomerization on the polarity of the solvent was less pronounced in films that incorporated isolated grains (according to TEM data) or in denser coatings.

Similar behaviors were also observed in the reactions of carbon tetrachloride with olefins (II) and hydrocarbons (III). In contrast to isomerization (I), reactions (II) and (III) occurred at temperatures of 130–150°C only after the removal of oxygen. The selectivity of both reactions for main products was higher than 99%. At 150°C, the addition was accompanied by the formation of up to 1% of products of the replacement of a hydrogen atom at the allyl position by a chlorine atom or group (CCl_3).

An induction period was not observed in the reactions of CCl_4 at temperatures higher than that of isomerization. Figure 5 exemplifies the kinetic curves of carbon tetrachloride addition to 1-octene (II) at different packing densities of copper nanoparticles. The catalytic activity of films in reactions (II) and (III) exhibited an extremum as the packing density of nanoparticles on the surface was increased. As can be seen in Tables 2, 3 and Fig. 6, as well as in reaction (I), the maximum rates and specific activities were attained in films with a particle density of 4×10^{12} particle/cm^2. In nonpolar decane, the extremal dependence of the activity on the metal content was less pronounced at 130°C than in the more polar dichloroethane solvent; however, it became more pronounced as the temperature was increased.

The above data allowed us to conclude that, in all the test reactions, an increase in the polarity of the solvent enhanced the performance of nanoparticles organized as ensembles. According to the above concepts,

Table 1. The dependence of the rate of isomerization (I) on metal content at 110°C in various solvents (1 : 10 dilution; 0.1 ml; [3,4-dichloro-1-butene] = 0.84 mol/l)

Sputtering time, min	Number of particles $\times 10^{-12}$, particle/cm^2	Film surface area, cm^2	Amount of copper,* mol Cu $\times 10^9$	Rate of isomerization, $r \times 10^2$, mol l^{-1} h^{-1}			Yield of 1,4-dichloro-2-butene in 2 h, %		
				dichloroethane ($\varepsilon = 10.03$)	chloroform ($\varepsilon = 5.05$)	carbon tetrachloride ($\varepsilon = 2.24$)	dichloroethane	chloroform	carbon tetrachloride
0.2	0.16	1.0	0.27	0.8	0.4	0.2	2	1	0.5
0.5	0.4	0.6	0.40	1.3	0.8	0.4	3	2	1
1	0.8	0.4	0.53	2.5	1.3	0.8	6	3	2
5	4	0.2	1.3	8.4	2.5	0.9	20	6	2
10	8	0.2	2.6	7.6	1.7	1.3	18	4	3
15	12	0.2	3.9	2.9	1.3	0.8	7	3	2

* To calculate the amount of copper in the catalyst with a known density of particle deposition, we assumed that one particle contains 10^3 copper atoms.

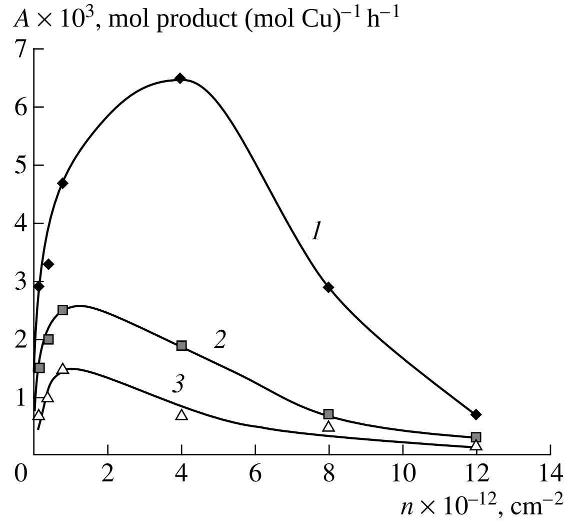

Fig. 4. The dependence of the specific catalytic activity (*A*) in 3,4-dichloro-1-butene isomerization at 110°C on surface metal particle density (*n*) in different solvents (1 : 10 dilution; 0.1 ml; [3,4-dichloro-1-butene] = 0.84 mol/l): (*1*) dichloroethane, (*2*) chloroform, and (*3*) carbon tetrachloride.

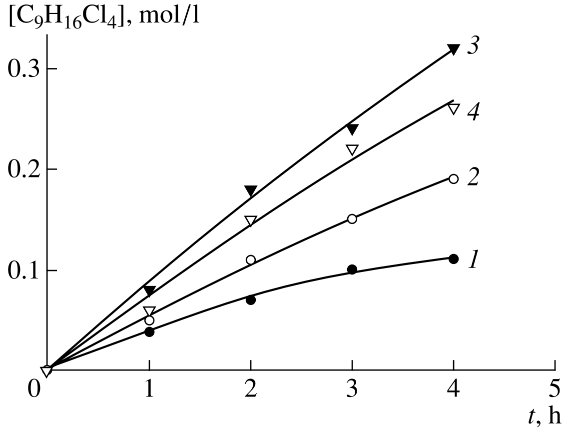

Fig. 5. Kinetic curves of 1,1,1,2-tetrachlorononane buildup in the addition of CCl_4 to 1-octene (0.2 ml of a solution with a volume ratio of 10 : 1; $[C_8H_{16}]$ = 0.57 mol/l) at 150°C and different deposition times, copper particle densities on the support, and catalyst film sizes, respectively: (*1*) 0.5 min, 0.4 × 10^{12} particle/cm^2, and 1 cm^2; (*2*) 1 min, 0.8 × 10^{12} particle/cm^2, and 0.5 cm^2; (*3*) 5 min, 4.0 × 10^{12} particle/cm^2, and 0.2 cm^2; and (*4*) 10 min, 8.0 × 10^{12} particle/cm^2, and 0.2 cm^2.

an increase in the catalytic properties of aggregated structures, which are characterized by a maximum activity, with the permittivity of the solvent at elevated temperatures can be due to the formation and stabilization of charged particles in closely packed monolayer films. The permittivity dependence of the catalytic properties of isolated nanoclusters and films with denser polylayer coatings was less pronounced.

The performance of catalyst samples with an optimum composition (~10^4 mol product (mol Cu)$^{-1}$ h^{-1}) was higher than that of traditional supported copper catalysts by several orders of magnitude; for example, the activity of the latter catalysts in reaction (I) was no higher than 200 even in the absence of a solvent [9]. We performed experiments on the addition of CCl_4 to 1-octene at 130°C with a supported copper catalyst prepared by a cryochemical synthesis in accordance with the published procedure [13]. The yields of 1,1,1,3-tetrachlorononane (at ~90% selectivity) were 52 and 35% in dichloroethane and decane, respectively (0.1 ml of a solution with $[C_8H_{16}]$ = 0.57 mol/l and 0.01 g of 5 wt % Cu/SiO_2, [Cu] = 7.8 × 10^{-3} mol/l). The activities in reaction (II) estimated from these data were 19 and 13 mol product (mol Cu)$^{-1}$ h^{-1}, respectively. These values are much lower than the values observed with copper nanoparticles prepared by laser electrodispersion, although TEM data suggest that the particle size in the cryochemically synthesized catalyst was about 10 nm. Previously, high activities were found only in the nanocomposites of copper in poly(*para*-xylylelne) at a certain composition near a percolation threshold when, as

Table 2. The dependence of the rate of reaction (II) between carbon tetrachloride and 1-octene on metal content at 130°C in various solvents (0.1 ml of a solution with the volume ratio solvent : CCl_4 : C_8H_{16} = 5 : 5 : 1; $[C_8H_{16}]$ = 0.57 mol/l)

Sputtering time, min	Number of particles × 10^{-12}, n/cm^2	Film surface area, cm^2	Amount of copper, mol Cu × 10^9	Rate of reaction, $r \times 10^2$, mol^{-1} l^{-1} h^{-1}			Yield of $C_9H_{16}Cl_4$ in 2 h, %		
				dichloroethane (ε = 10.03), 130°C	decane (ε = 2), 130°C	decane (ε = 2), 150°C	dichloroethane, 130°C	decane, 130°C	decane, 150°C
0.5	0.4	1.0	0.65	3.4	1.4	2.9	12	5	10
1	0.8	0.6	0.80	5.7	1.7	5.4	20	6	19
3	2.4	0.3	1.2	8.3	2.8	9.4	29	10	33
5	4	0.2	1.3	10.3	4.3	14.0	36	15	49
10	8	0.2	2.6	9.4	2.6	10.0	33	9	35
15	12	0.2	3.9	2.6	1.1	–	9	4	–

Table 3. The dependence of the rate of reaction (III) between carbon tetrachloride and decane on metal content at 150°C and a volume ratio of 1 : 1 (0.1 ml, $[CCl_4] = 5.3$ mol/l; $[C_{10}H_{22}] = 2.6$ mol/l)

Sputtering time, min	Number of particles $\times 10^{-12}$, n/cm^2	Film surface area, cm^2	Amount of copper, mol Cu $\times 10^9$	Rate of reaction, $r \times 10^2$, mol l^{-1} h^{-1}	Yield of $C_{10}H_{21}Cl$ in 2 h, %
0.5	0.4	0.6	0.40	0.5	0.4
1	0.8	0.4	0.53	0.9	0.7
3	2.4	0.3	1.2	2.3	1.8
5	4	0.2	1.3	3.0	2.3
10	8	0.2	2.6	1.7	1.3
15	12	0.2	3.9	1.0	0.8

in the given case, conditions were provided for the interaction of nanoparticles with each other [8, 9].

Thus, we can say that the unusually high activity of nanoparticles organized as ensembles is, probably, a consequence of the interaction between individual aggregates, and it can be considered as a common feature of the catalytic behavior of the ensembles of interacting nanoparticles. Different effects of the permittivity of the solvent on the increase in the catalytic properties of isolated nanoclusters, their aggregates, and closely packed films are due to different fractions of charged grains depending on the distribution of particles on the surface or in the matrix. Films with grain aggregates in which the probability of electron tunneling between closely spaced granules and, correspondingly, the appearance of charged grains dramatically increased with ε are most sensitive to changes in the polarity of the solvent. The experimental data support the occurrence of a size effect of the second kind. Indeed, with a constant particle size, the metal surface area S is linearly related to n and the weight of the metal. In this case, it has no effect on the specific activity A based on unit weight; consequently, the dependence of A on n is not related to changes in particle size (it is constant) or S. The only parameter that affects the activity is the value of L, the change of which is responsible for the observed extremal functions.

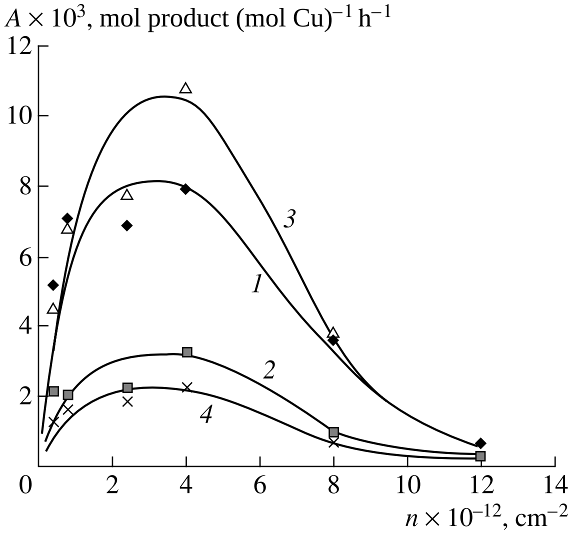

Fig. 6. The dependence of the specific catalytic activity (A) on surface metal particle density (n) in different solvents in the reactions of carbon tetrachloride with 1-octene (0.1 ml of a solution with the volume ratio solvent : CCl_4 : C_8H_{16} = 5 : 5 : 1; $[C_8H_{16}] = 0.57$ mol/l; (*1*) dichloroethane, 130°C; (*2*) decane, 130°C; and (*3*) decane, 150°C) or (*4*) decane at 150°C and a 1 : 1 volume ratio (0.1 ml; $[CCl_4] = 5.3$ mol/l; $[C_{10}H_{22}] = 2.6$ mol/l).

A common feature of the test reactions is that, probably, electron transfer from a metal particle to an organochlorine substrate took place at the first step of the reaction with the formation of an organochlorine radical anion:

$$M_n + RCl \longrightarrow M_n^+ + RCl^{\overset{\bullet}{-}}.$$

This transfer was facilitated on the appearance of negative charges on interacting nanoparticles in nanoparticle aggregates. The nature of the induction period of reaction (I) remains unclear. A study of catalysts after the reaction with the use of scanning electron microscopy demonstrated that the particle size and distribution on the surface of the support remained unchanged. We can only assume that, under exposure to the reagent, the chemical composition of the catalyst was affected and a more active structure was formed, which facilitated electron transfer from the catalyst to the substrate. It is likely that, after the electron transfer, the unstable halogen-containing radical anion decomposed to form a radical $R^\bullet$ and a Cl^- anion. It is likely that because of this the oxide layer of nanoclusters was enriched in a metal chloride. The radical $R^\bullet$ participated in the subsequent transformations to form the products of reactions (I)–(III) on the catalyst surface or in solution. The yield of radical species in solution and the radical-chain character of processes are most probable for reactions (II) and (III), which occur only in the absence of oxygen, which is an inhibitor of chain reactions with the participation of haloalkyl radicals [14].

In general, the most important characteristics of the catalysis of the reactions of halogen derivatives by structurally organized nanocomposites—the anomalously high catalytic activity, the extremal dependence of the activity on metal content and distance between nanoparticles, and the specific dependence of the reaction rate on the permittivity of the solvent—are consistent with concepts of the key role played by interacting nanoparticle ensembles.

ACKNOWLEDGMENTS

This work was supported by the Russian Foundation for Basic Research (project nos. 01-02-17827, 02-03-32609, and 03-03-06030) and the federal special program *Integratsiya* (B0061).

REFERENCES

1. Coq, B. and Figueras, F., *Coord. Chem. Rev.*, 1998, vols. 178–180, p. 1753.
2. Henry, C.R., *Appl. Surf. Sci.*, 2000, vol. 164, p. 252.
3. Stakheev, A.Yu. and Kustov, L.M., *Appl. Catal.*, 1999, vol. 188, p. 3.
4. Vorontsov, P.S., Gerasimov, G.N., Golubeva, E.N., Grigor'ev, E.I., Zav'yalov, S.A., and Trakhtenberg, L.I., *Zh. Fiz. Khim.*, 1998, vol. 72, no. 10, p. 1742.
5. Trakhtenberg, L.I., Gerasimov, G.N., Grigoriev, E.I., Zavjalov, S.A., Zufman, V.Yu., and Smirnov, V.V., *Stud. Surf. Sci. Catal.*, 2000, vol. 130, p. 941.
6. Trakhtenberg, L.I., Gerasimov, G.N., Grigor'ev, E.I., Zav'yalov, S.A., Zagorskaya, O.V., Zufman, V.Yu., and Smirnov, V.V., *Zh. Fiz. Khim.*, 2000, vol. 74, no. 5, p. 955.
7. Zagorskaya, O.V., Zufman, V.Yu., Rostovshchikova, T.N., Smirnov, V.V., and Gubin, S.P., *Izv. Akad. Nauk, Ser. Khim.*, 2000, no. 5, p. 854.
8. Trakhtenberg, L.I., Gerasimov, G.N., Potapov, V.K., Rostovshchikova, T.N., Smirnov, V.V., and Zufman, V.Yu., *Vestn. Mosk. Univ., Ser. 2: Khim.*, 2001, vol. 42, no. 5, p. 325.
9. Vorontsov, P.S., Grigor'ev, E.I., Zav'yalov, S.A., Zav'yalova, L.M., Rostovshchikova, T.N., and Zagorskaya, O.V., *Khim. Fiz.*, 2002, vol. 21, no. 2, p. 45.
10. Rostovshchikova, T.N., Smirnov, V.V., and Kokorin, A.I., *J. Mol. Catal., A: Chem.*, 1998, vol. 129, nos. 2–3, p. 141.
11. Tarkhanova, I.G., Smirnov, V.V., and Rostovshchikova, T.N., *Kinet. Katal.*, 2001, vol. 42, no. 2, p. 216.
12. Kozhevin, V.M., Yavsin, D.A., Kouznetsov, V.M., Busov, V.M., Mikushkin, V.M., Nikonov, S.Yu., Gurevich, S.A., and Kolobov, A., *J. Vac. Sci. Technol. B.*, 2000, vol. 18, no. 3, p. 1402.
13. Kondakov, S.E. and Smirnov, V.V., *Kinet. Katal.*, 1995, vol. 36, no. 3, p. 348.
14. Sergeev, G.B. and Smirnov, V.V., *Molekulyarnoe galogenirovanie olefinov* (Molecular Halogenation of Olefins), Mosk. Gos. Univ., 1985, p. 147.